Journal of the Nigerian Association of Mathematical Physics
Volume34,(*March, 2016*), pp 323 – 330

Simulation of Positron Beam Driven Plasma Wakefield Acceleration Using the Particle-In-Cell Code in Metre-Scale Plasma

Gangtak N., [2]Anchaver R.S. and [3]I.M.Echi

[1]GSS Bassa, Bassa Area Directorate, Plateau State Ministry of Education, Plateau state, Nigeria.
[2]Department of Physics, Benue State University, P.M.B. 102119, Makurdi, Nigeria.
[3]Department of Physics, University of Agriculture Makurdi, P.M.B.2373, Makurdi, Benue State, Nigeria.

Abstract

This paper presents a plasma wakefield acceleration scheme driven by positron beam using the particle-in-cell simulation code in two dimensions. A $30GeV$ ***positron beam of*** $500pC$ ***charge,*** $75\mu m$ ***long beam and a transverse size of*** $20\mu m$ ***is propagated through a*** $1m$ ***long plasma with initial density of*** $3\times10^{21}m^{-3}$***. The particles in the plasma were variably weighted to represent the density ramp. The initial beam density was set to a value greater than the plasma density and the beam propagation followed the magnetically self-focused regime. Results show that as the beam entered the plasma, the plasma wakefield was excited as a result a strong axial electric field gradient (accelerating gradient) slightly in excess of*** $2.9GV/m$***.When the plasma density was increased from*** $3\times10^{21}m^{-3}$ ***to*** $6\times10^{21}m^{-3}$***, the accelerating field gradient increased up to*** $4.1GVm^{-1}$***. The peak self-focusing magnetic field gradient (B-field) achieved was about*** $0.62\ T/m$***. This value was sufficient enough to induce noticeable plasma density perturbation which in turn enhanced the positron beam acceleration.***

Keywords: Positron beam, beam density, plasma density, axial electric field, focusing field, wakefield.

1.0 Introduction

Due to the limitations of conventional accelerators,several attempts have been made to use plasma in place of metallic walls of the conventional accelerators to accelerate charged particles to high energies. The energy requirements in the present day frontier of high energy Physics is several trillion electron volts. To build conventional accelerators (suchas the Large Hadron Collider(LHC) and the International Linear Collider (ILC)) in this energy regime is very expensive and time consuming. Many of such projects are often abandoned midstream due to funding constraints. It is therefore imperative to explore new methods of accelerating charged particles to high energies [1]. Plasma have extraordinary potentials for advancing the energy frontier in high energy physics due to the large focusing and accelerating fields that are generated[2]. Plasma can sustain high electric field gradient which ordinarily will melt the conventional accelerator's components. Typical breakdown due to electric field gradient of $100MeVm^{-1}$ has been reported in the literature [3]. Enhanced plasma-based accelerator schemes utilizing relativistically propagating plasma waves have been under active investigation because of their potentials to accelerate charged particles at gradients that are order of magnitude greater than those currently employed in radio frequency cavitiesconventional colliders [4 -7].

The ultimate utility of plasma accelerators will depend on sustaining ultrahigh accelerating fields over a substantial length to achieve significant energy gain. Impressive gradient much in excess of $1GeVm^{-1}$, $2.0GVm^{-1}$ and the energy gain of $2.7GeV$, $\lesssim 100MeV$ have been obtained but only over plasma lengths of $< 1cm, 13cm, 10cm$respectively [4,2,9,10].Where the plasma length could be appreciable (1.4m), the energy gain is drastically very low ($192MeVm^{-1}$)[8]. Plasma density fluctuations have been known to enhance the strength of the accelerating electric field. Accelerating field gradient of$3.2\times10^{11}Vm^{-1}$ at low density and$5.2\times10^{11}Vm^{-1}$ at high density ramp have been reported [11].

The essence of this paper is to use the particle-in-cell (PIC) simulation to achieve high accelerating field gradient in$1m$ long plasma with positrons as the drive beam. Such a plasma length will be sufficient enough for the drive beam to significantly

Corresponding author: Gangtak N., E-mail:pgangtak@gmail.com, Tel.: +2348160643107

lose its energy to the wakefield.Our results may significantly impact on the applicability of plasma acceleration scheme to high energy accelerators.

2.0 Theoretical Consideration

2.1 Plasma Wave Generation

The physical factor responsible for generating plasma waves in a plasma wakefield acceleration scheme is the space charge force of the drive beam. When the positron propagates into the background plasma, the beam density n_b generates a space charge potential via Poisson's equation [12]

$$\nabla^2\phi = k_p^2\left(\frac{n}{n_0}+\frac{n_b}{n_0}-1\right) \quad (1)$$

Where n is the electron plasma density, n_0 is the uniform plasma density, ϕ is the electric potential and $k_p^2 = \frac{\omega_p^2}{c^2}$. The space charge force required to drive the plasma wake is given by

$$F = -mc^2\nabla\phi \quad (2)$$

Consider that $n_b \ll n_0$ and if the radius of the beam is $r_b \gg \lambda_p$, then equation (1) reduces to the form

$$\nabla^2\phi = k_p^2\left(\frac{n}{n_0}-1\right) \quad (3)$$

The plasma electrons will respond to the space charge potential of the beam, thus the plasma density is perturbed($\delta n = -n_b$). That is the beam density has a perturbation effect on the electron plasma density. Therefore if the beam terminates in a period less than ω_p^{-1}, a wakefield (charge density oscillation) of the form of equation (4) is generated

$$\delta n = n_b sink_p(z-ct) \quad (4)$$

But the axial electric field gradient due to the wakefield behind the drive beam is given by

$$\frac{\partial E_z}{\partial z} = -4\pi e\delta n \quad (5)$$

Substituting equation (4) into (5) yields

$$\frac{\partial E_z}{\partial z} = -4\pi e n_b sink_p(z-ct) \quad (6)$$

Integrating equation (6) yields

$$E_z = 4\pi e\frac{n_b}{k_p}cosk_p(z-ct) \quad (7)$$

Equation (7) describes the longitudinal component the longitudinal component of the wakefield behind the drive beam. Thus the peak amplitude of the wake is given by

$$E_{max} = \left(\frac{n_b}{n_0}\right)E_0 \quad (8)$$

whereE_0 is the nonrelativistic wave-breaking field given by

$$E_0 = \frac{cm_e\omega_p}{e} \quad (9)$$

where c is the speed of light, m_e is the mass of electron, ω_p is the plasma frequency and e is the elementary charge.

To account for the self-consistent transverse electric and the self-focussing magnetic fields the full Maxwell electromagnetic equations have to be used. That is

(10)

(11)

The field solutions of these equations are used in pushing particles in accordance with the Newton-Lorentz laws:

(12)

2.2 Particle-in-Cell Simulations

The particle-in-cell (PIC) simulation package Vsim (version 7.2) incorporating the Vorpal simulation engine is used to implement 2-D PIC simulations of the positron beam propagated through the plasma. The simulation package consists of an electromagnetic solver that uses the Yee algorithm and initBeam macro to set up the initial beam properties. The beam (positron beam) travels near the speed of light and Matched Absorbing Layers (MALs) are used on the transverse sides of the window to absorb outgoing waves. The plasma is represented by macro-particles and both the beam and plasma are moved using the Boris push. The plasma particles are variably weighted to represent density ramp. It is assumed the plasma consists of pre-ionized heavy ions, which do not move in the time frame of the simulations. The positron beam initializes the field using a speed of light frame Poisson equation solve, then the fields are evolved using Finite Difference Time Domain (FDTD) PIC [13]. That is an electrostatic solution in the bunch rest frame is performed, and the resulting electric field is

transformed to the plasma rest frame to provide the bunch's initial electromagnetic field. The electromagnetic fields are then updated in a FDTD scheme using the Yee algorithm. Vorpal initially loads the particles bunch onto a regular grid as an even distribution of variable-weight macro particles which helps to eliminate numerical instabilities due to density fluctuations [10].

The positron beam is launched from $x = 0$ in the positive x-direction using the Lorentz boosted Poisson fields to ensure that the simulation is self-consistent from start. The beam is allowed to propagate forward into a ramped plasma density distribution, and simulation runs for a specified number of time steps, with data dumped periodically to Hierarchical Data Format version 5 (HDF5) files – a file format for storing graphical and numerical data and for transferring data between computers. The basic PIC procedure is illustrated in Figure 1 while the input parameters are shown in Table 1.

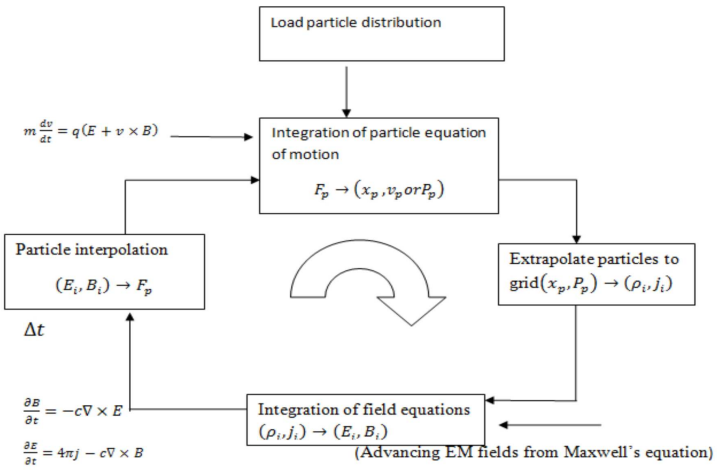

Figure 1: Flow chart of the simulation procedure

Table 1: Parameters used in this simulation

Parameter	Value
Plasma density $(n_p)3 \times 10^{21} m^{-3}$	
Number of plasma particles per cell	9
Number of cells $[\Delta x, \Delta y][128, 176]$	
Total number of cells	22528
Total number of plasma particles	202752
Number of beam particles per cell	16
Total number of beam particles	360448
Grid size [LX, LY]	$[12 \times 10^{-3}, 44 \times 10^{-4}]$
Beam density $(n_b)6.61 \times 10^{21} m^{-3}$	
Beam energy	$30GeV$
Beam charge	$500pC$
RMS Beam Length $(\sigma_z)75\mu m$	
RMS Beam Radius $(\sigma_r)20\mu m$	
Mass of positron	$9.1092 \times 10^{-31} kg$
Speed of light (C)	$2.9979 \times 10^{8} m/s$
Plasma length	$1m$
Plasma frequency	$3.255 \times 10^{7} s^{-1}$
Elementary charge $(e^+)1.6 \times 10^{-19} C$	
Pi $(\pi)3.142$	

3.0 Results and Discussion

Figure 2(a) shows the initial beam profile and the longitudinal wakefield in Cartesian coordinates. Here y – and x – axes are the transverse and longitudinal coordinates in metre containing the initial beam and wakefield profile before full propagation of the positron beam (FPPB) in the plasma, while (b) is the initial longitudinal electric field gradient cast on axis, where the transformer ratio is unity indicating that the beam has not lost its energy. To this end, the beam is stiff and its particles do not physically move.

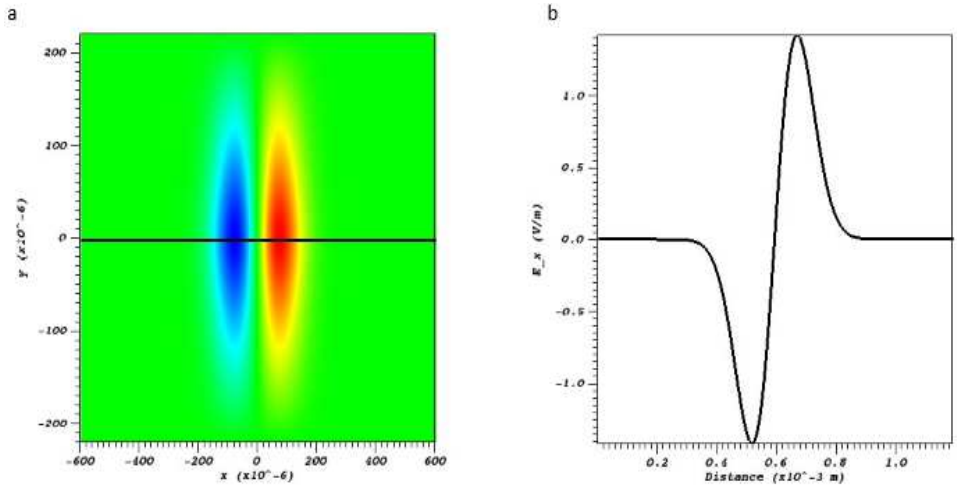

Figure 2: (a) The initial longitudinal wakefield and positron beam profile where the ovoid pink structure is the positron beam the blue structure is the wakefield. (b) the electric field gradient cast on axis.

Figure 3(a) shows the longitudinal wakefield profile as contour colour plot after FPPB in the plasma, where a periodic wakefield (space - charge oscillation or charge disturbance) is observed with a phase velocity$v \sim c$. In (b) is the longitudinal electric field gradient (accelerating field) cast on axis after FPPB through the plasma. The peak accelerating field is slightly in excess of $2.9GV/m$ which is greater than the one in literature [2,4, 8 -10].

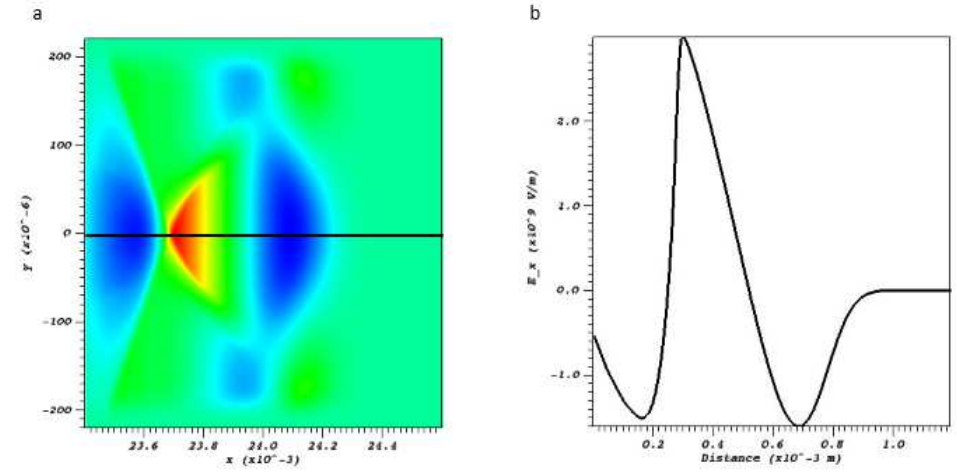

Figure 3:(a) the longitudinal wakefield profile as contour colour plot. (b) Longitudinal electric gradient after FPPB through the plasma.

Figure 4 is the vector profile of Figure 3(a) illustrating the effects of the beam's space charge on the plasma electrons after FPPB through the plasma, where the plasma electrons are pulled from different radii arrive at different time along the beam. The curves shown here are contour curves of various constant electric fields.

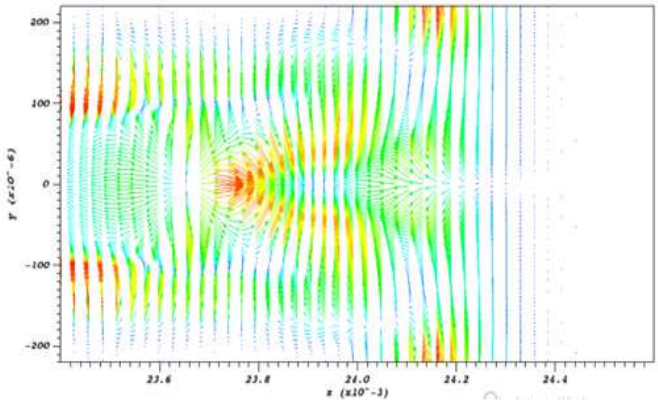

Figure 4: Vector profile of figure 3(a) (beam space charge (red), plasma electrons and wakefield behind the beam (green)).

Figure 5 is an overlay (superimposition) of the colour contour plot of longitudinal wakefield profile (Figure 3(a)) on its vector profile (Figure 4) depicting clearly the charge disturbance behind the beam, plasma electrons sucked in from different distance within the plasma and some electrons trapped by the beam and get accelerated as well.

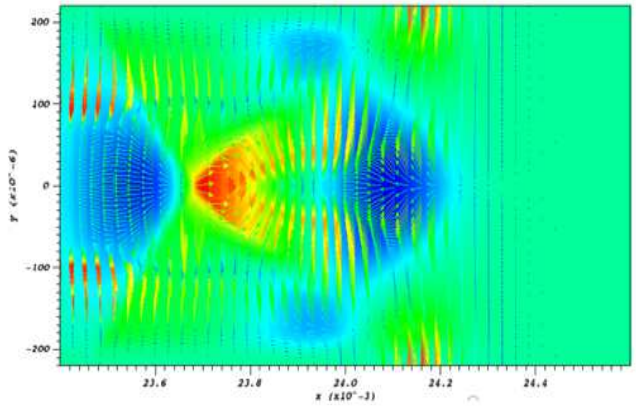

Figure 5: Overlay of the longitudinal wakefield profile on its vector profile after FPPB through the plasma.

Figure 6(a) shows the unperturbed longitudinal plasma density profile before FPPB, while (b) is the unperturbed plasma density cast on axis before FPPB through the plasma. This reveals that the plasma density is not perturbed until the beam is propagated in the plasma as revealed by Figure 7.

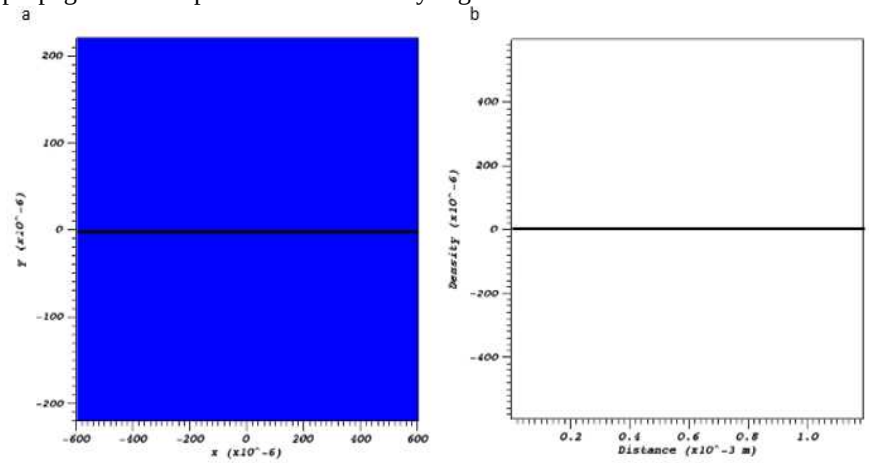

Figure 6: (a) Longitudinal unperturbed plasma density profile. (b) Longitudinal plasma density profile cast on axis.

Figure 7(a) shows the colour contour profile of the longitudinal perturbed plasma density after FPPB through plasma .This indicates a strong charge density behind the beam which result in a spike of the electric field components. (b) Shows the perturbed plasma density profile cast on axis after FPPB through the plasma.

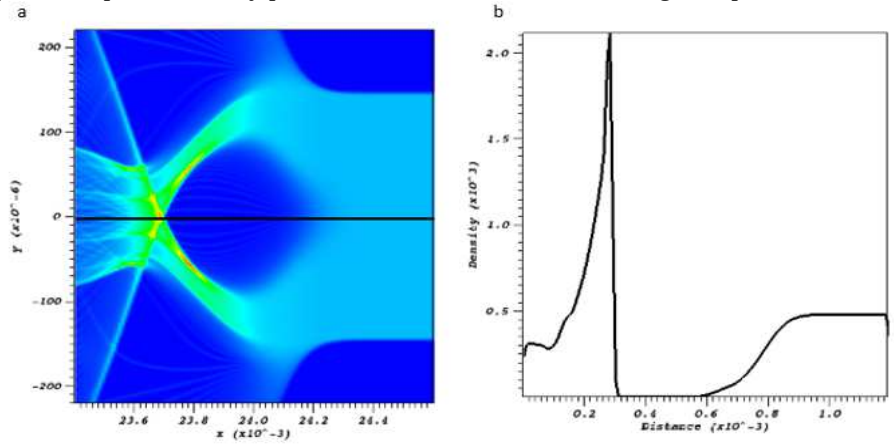

Figure 7: (a) the perturbed plasma density profile after FPPB through the plasma. (b) Theperturbed plasma density profile cast on axis.

Figure 8(a) is the longitudinal wakefield as colour contour plot, while (b) the electric field gradient after FPPB through the plasma when plasma density is increased from $3 \times 10^{21} m^{-3}$ to $6 \times 10^{21} m^{-3}$while other parameters remain constant. The peak electric field gradient (accelerating field) is $\gtrsim 4.1 GV/m$. The increase in the accelerating field gradient may be due to the high level of nonlinearity in the wakefield as suggested by it non-sinusoidal nature when compared to that of figure 3(a). Also comparing Figures 7 and 9, one sees that the plasma density is more perturbed in Figure 9 (when the plasma density was increased) than in Figure 7 (when the density was low). This implies that plasma density fluctuation may be another reason for the increase in the accelerating gradient similar to the findings in [11].

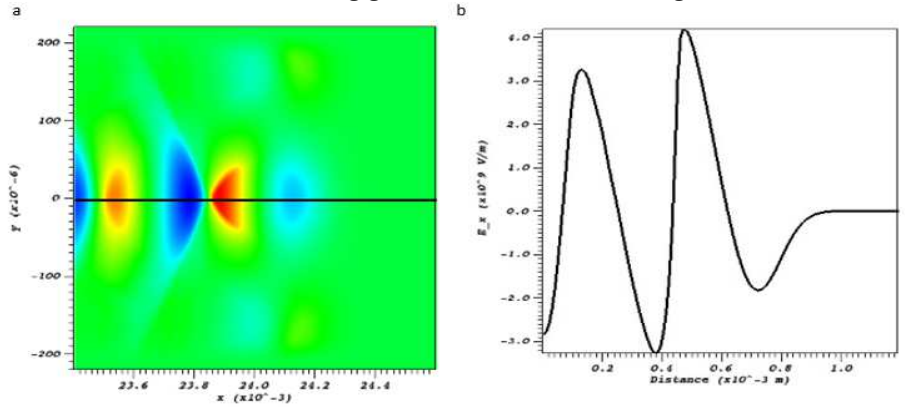

Figure 8: (a) the longitudinal wakefield profile as contour colour plot and (b) longitudinal electric gradient after FPPB through the plasma at the plasma density $6 \times 10^{21} m^{-3}$.

Figure 9(a) is the colour contour profile of the longitudinal perturbed plasma density after FPPB through plasma and (b) shows the perturbed plasma density profile cast on axis after FPPB through the plasma at initial density of $6 \times 10^{21} m^{-3}$.

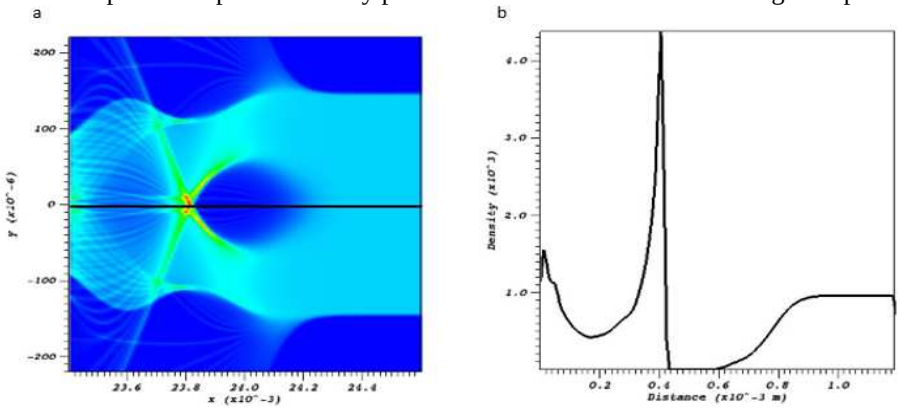

Figure 9: (a) the perturbed plasma density profile after FPPB through the plasma and (b) the perturbed plasma density profile cast on axis at $6 \times 10^{21} m^{-3}$.

Figure 10(a) shows the longitudinal profile of the magnetic field (focusing field) as colour contour plot, while (b) is the longitudinal profile of the field cast on axis after FPPB through the plasma.

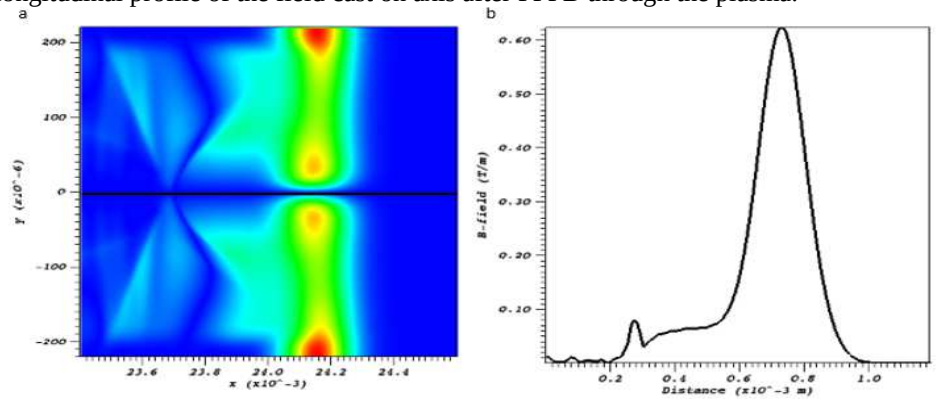

Figure 10: (a) Longitudinal profile of the magnetic field. (b) Longitudinal profile of magnetic field cast on axis.

From Figure 10b, the peak value of the self-focusing B-field is about $0.62Tm^{-1}$. This value is sufficient enough to cause the plasma density ramp observed in Figure 9b. It is practically intuitive that the more focus a traversal beam is, the more density fluctuation it can induce on the host plasma since the plasma electrons will have longer distances to move before reaching the of beam propagation.

Figure 11 is the phase space plot of the drift velocity of the beam in m/s against the longitudinal distance in m, showing the resulting acceleration of the positron beam particles after FPPB through the plasma.

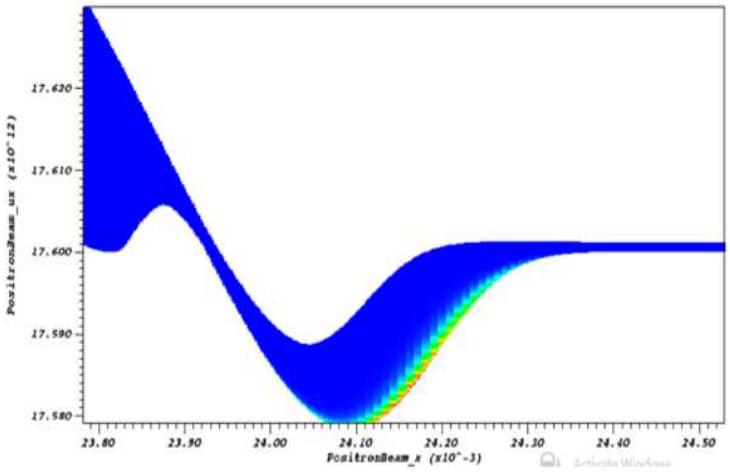

Figure 11: Illustrates the resulting acceleration of the beam particles after FPPB.

4.0 Conclusion

The main results of the interactions of positron beam with the plasma in a plasma wakefield acceleration scheme has been considered. The beam/plasma parameters used in this simulation yields an accelerating gradient slightly in excess of $2.9GV/m$. But when the plasma density was increased from $3 \times 10^{21}m^{-3}$ to $6 \times 10^{21}m^{-3}$ while other parameters remain unchanged, a sudden increase in accelerating gradient slightly in excess of $4.1GV/m$ is achieved. Also the plasma density is perturbed when the beam is propagated in the plasma otherwise the plasma density remains unperturbed. This suggests that the positron beam parameters used will yield high accelerating gradient when propagated in plasma of appropriate density.

5.0 Acknowledgements

We acknowledge Tech-X Corporation for allowing the use of their code (Vsim, version 7.2)

6.0 References

[1] Blumenfeld I., Clayton E.C., Decker F.-J., Hogan M.J., Huang C., Rasmus I., Iverson R., Joshi C., Katsouleas T., Neil K., Wei L., Marsh K.A., Mori W.B., Muggli P., Erdem., Siemann R.B., and Walz D. (2007). Energy doubling of $42GeV$ electrons in a metre-scale plasma wakefield accelerator. *Submitted to Nature* .SLAC-PUB-12363.

[2] Hogan M.J., Clayton C.E., Decker F.J., Deng S., Emma P., Huang C., Iverson R.H., Johnson D.K., Joshi C., Katsouleas T., Krejcik P., Lu W., Marsh K.A., Mori W.B., Muggli P., O'Connell C.L., Oz E., and Seimann R.H.,(2006). Multi-GeV energy gain in a plasma-wakefield accelerator.*Submitted to physical Review Letters.*SLAC-PUB-11383

[3] James A.H. (2010) simulating plasma wakefield acceleration. M.sc. thesis.Department of physics.Imperial college. London.

[4] Hogan M.J., Assman R., Decker F.-J., Iverson R., Raimondi P., Rokni S., Seimann R.D., Walz D., Whittum D., Blue B., Clayton C.E., Dodd E., Hemker R., Joshi C., Marsh K.A., Mori W.B., Katsouleas T., Lee S., Muggli P., Castravas P., Chattopadhyay S., Esarey E., and Leemans W.P. (2000). E-157: A 1.4-m-long plasma wake field acceleration experiment using a 30GeV electron beam from the Stanford Linear Accelerator Center Linac. *Physics of Plasmas.* 7(5): 2241-2248

[5] Tajima T., and Dawson M.C. (1979). Laser electron accelerator.*Physical Review Letters.* 43:267-270

[6] Chen P., Dawson J.M., Huff R.W., andKatsouleas T. (1985). Acceleration of electron by the interaction of a bunched electron beam with plasma.*Physical Review Letters.* 54: 693-696.

[7] Joshi C., Mori W.B., Katsouleas T., Dowson J.M., Kindel J.M., and forlund D.W. (1984). Ultrahigh gradient particle acceleration by intense laser-driven plasma density waves.*Nature.* 311:525-529.

[8] Baird K., Decker F.-J., Hogan M.J., Iverson R.H., Raimondi P., Siemann R.H., Walz D., Blue B.E., Clayton C.E., Dodd E.S., Joshi C., Marsh K.A., Mori W.B., Wang S., Katsouleas T., Lee S., Muggli P., Assmann R. (2000). E162, positron and electron dynamics in a plasma wakefield accelerator. *SLAC-ARDB*-242

[9] Haruna M.A. and Anchaver (2013) simulation of position beam driven plasma wakefield acceleration using the particle-in-cell code, OOPIC. *Journal of the Nigerian Association of mathematical Physics*. 25: 129-134

[10] Hanahoe K., Mete O., Xia G., Angal-Kalinin D., Clarke J., Jones J., McKenzie J.W., Militssyn B.L., Williams P., Smith J., Welsch C., Wei Y.,Hidding B. (2014). Plasma acceleration at CLARA PARS.*Proceedings of ipac 2014 Dresden*, Germarypp 1544-1456

[11] Jaehoon K., Geun J.K., and Seong H.Y. (2011). Energy enhancement using an upward density ramp in laser wakefield acceleration. *Journal of the Korean physical society*. 59(5):3166-3170

[12] Eric E., Sprangle P., Jonathan K., Antonio T. (1996) Overview of plasma-Based accelerator concepts. *IEEE Transactions on plasma Science*. 24 (2): 256-259

[13] Tech-X Corporation, www.txcorp.com/home/vsim/vsm -documentation.